

Reprinted from

APPLIED PHYSICS EXPRESS

Collimated Field Emission Beams from Metal Double-Gate Nanotip Arrays Optically Excited via Surface Plasmon Resonance

Patrick Helfenstein, Anna Mustonen, Thomas Feurer, and Soichiro Tsujino

Appl. Phys. Express **6** (2013) 114301

Collimated Field Emission Beams from Metal Double-Gate Nanotip Arrays Optically Excited via Surface Plasmon Resonance

Patrick Helfenstein^{1†}, Anna Mustonen^{1†}, Thomas Feuerer², and Soichiro Tsujino^{1*}

¹Laboratory for Micro- and Nanotechnology, Paul Scherrer Institut, 5232 Villigen, Switzerland

²Institute of Applied Physics, University of Bern, 3012 Bern, Switzerland

E-mail: soichiro.tsujino@psi.ch

Received August 23, 2013; accepted September 22, 2013; published online October 15, 2013

The generation of collimated electron beams from metal double-gate nanotip arrays excited by near infrared laser pulses is studied. Using electromagnetic and particle tracking simulations, we showed that electron pulses with small rms transverse velocities are efficiently produced from nanotip arrays by laser-induced field emission with the laser wavelength tuned to surface plasmon polariton resonance of the stacked double-gate structure. The result indicates the possibility of realizing a metal nanotip array cathode that outperforms state-of-the-art photocathodes. © 2013 The Japan Society of Applied Physics

The use of field emission sources for atomic-resolution electron microscopy¹ has motivated research on their application to free-electron lasers (FELs)^{2–4} and THz vacuum electronic devices^{5–8} that demand current and beam brightness higher than conventional cathodes. The requirements for cathodes are most stringent for X-ray FELs since their radiation power and shortest wavelength largely depend on the electron beam quality at the cathode. In the case of the SwissFEL X-ray FEL being constructed at the Paul Scherrer Institute, the cathode should generate 200 pC electron pulses with 10 ps duration with an intrinsic transverse emittance below 0.2 mm-mrad,³ and it should be compatible with the acceleration field in the order of 100 MV/m in order to minimize the space charge effect during the initial acceleration of the electron pulses.⁹ Existing and planned X-ray FELs commonly employ photocathodes excited by UV laser that produce electron beams with the brightness approaching a theoretical limit.¹⁰ Hence, whether one can utilize the high brightness of field emission sources to realize a cathode that outperforms state of the art photocathodes is an urgent question with a potential impact on the X-ray FEL technology in the near future. For this purpose, we propose double-gate field emitter arrays (FEAs) with on-chip electron extraction (G_{ex}) and collimation (G_{col}) gate electrodes excited by near infrared (NIR) laser pulses.

To increase the total current, FEAs combine electron emission from a large number of nanotip emitters.^{6,11,12} The generation of field emission current up to 0.4 A from a single-gate Spindt FEA¹¹ and current of ~ 0.6 A from diamond FEAs without gate electrodes¹³ induced by electrical potential in dc or microsecond pulse has been reported. However, to fulfill the X-ray FEL cathode specification, it is mandatory to achieve higher emission current with shorter pulse duration, as well as an order of magnitude decrease of the electron velocity spread in the direction transverse to the axis of the electron gun.^{14,15} Recent experiments indeed showed that the intrinsic transverse beam emittance of FEAs of 1 mm diameter is 1–3 mm-mrad,^{16,17} corresponding to the rms transverse velocity u_t of $\sim 3 \times 10^{-3} c$ (c is the speed of light in vacuum), which has to be reduced by more than an order of magnitude to be compatible with the X-ray FEL requirement.

To generate short electron pulses, NIR laser pulse excitation of metal FEAs has been proposed and experimentally studied.^{18,19} Up to 5 pC electron pulses were generated from a 10^5 -tip single-gate FEA with a 5 μm array pitch excited by 50 fs NIR laser pulses with the wavelength of 800 nm.¹⁹ To produce higher charge pulses, for example with the charge of 200 pC to match the SwissFEL requirement, the yield of the FEA has to be increased to minimize the beam emittance by keeping the array size the same or smaller. One of the promising ways proposed recently is to increase the tip density by reducing the array pitch below 1 μm and to tune it so that the surface plasmon polariton (SPP) of the gate electrode is in resonance with the photon energy of the illuminating NIR pulses.²⁰ The simulation showed that the extraordinary optical transmission (EOT)²¹ persists in the presence of molybdenum emitters, and the electron yield reaching 10^{-6} was predicted.²⁰ Since the laser-induced field emission from metal emitters is localized at the nanometer-size tip apex,^{19,22–24} one can expect to reduce u_t of the laser-excited electron beams in a double-gated structure^{25–30} as demonstrated in recent experiments.^{28,30}

In this work, we therefore explore the feasibility of FEAs for the advanced accelerator applications by combining the recent developments on the NIR laser excitation of FEAs and the double-gate technology. In particular, by using three-dimensional electromagnetic and particle tracking simulations, we study the NIR laser-induced field emission from double-gate FEAs with plasmonic gate electrodes and their beam collimation characteristics.

The proposed device is schematically shown in Figs. 1(a) and 1(b). To analyze its operation, we used a three-dimensional double-gate emitter model shown in Figs. 1(c) and 1(d). We assumed a cone shaped molybdenum emitter terminated by a spherical apex with the radius of curvature (R_{tip}) of 5 nm. The aperture diameter of G_{ex} was 200 nm and the aperture diameter of G_{col} was 600 nm. The large G_{col} aperture diameter is a key to suppress the current reduction when the collimation is strongest at large negative collimation potential V_{col} applied between G_{col} and G_{ex} while extracting the electrons from the emitters by applying the extraction potential V_{ge} between G_{ex} and the emitter substrate (Em) [see Fig. 1(b)].^{28,30} We set the external acceleration field F_{acc} of 100 MV/m, a typical value for RF cavity photoinjector.¹⁰ The material of the gate electrodes

[†]These authors contributed equally to this work.

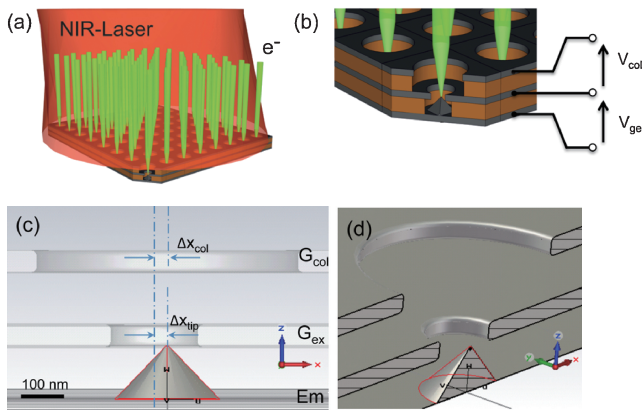


Fig. 1. (a) Generation of high-charge and low-emittance electron pulses from a double-gate metal nanotip array excited by NIR laser pulses. (b) Close-up view of the proposed device. (c) and (d) show the cross-sectional views of the model along the $y = 0$ plane, from the side and oblique angle, respectively. The height and the base radius of the emitter are 120 nm. The thickness of the gate layers is 50 nm. The separations between G_{ex} and Em and between G_{ex} and G_{col} are 120 nm.

was assumed to be copper since it can not only support SPP at optical frequencies but it is also compatible with the high F_{acc} . In the particle tracking and electrostatic simulation, we included F_{acc} in the model by placing an anode at a distance of $1.5 \mu\text{m}$ above G_{col} and assumed its potential equal to 150 V, while fixing the potential of G_{col} to ground potential. From the electron distribution at the anode, u_t of the double-gate emitter was evaluated. For simplicity, the insulator layers that support the gate layers mechanically in actual devices were replaced by vacuum in the simulation.

To calculate the optical electromagnetic field distribution, we used a finite element electromagnetic solver (COMSOL Multiphysics, RF module³¹⁾) with adaptive tetragonal meshing. To simulate the laser excitation of a large array, we assumed a 750-nm-wide cuboidal unit cell and applied the periodic boundary condition in the transverse direction. The dielectric functions of the emitter and gate layers were taken from Ref. 32. The array pitch of 750 nm was chosen to set the expected EOT resonance through the gate layers close to the wavelength of 800 nm.¹⁹⁾ A finite shift Δx_{tip} of the tip position from the center of G_{ex} is crucial to have the optical electric field F_{op} at the tip apex several times higher than the optical electric field F_0 of the incident field as shown previously in the case of single-gate FEAs.^{20,33)} In the present simulation, we assumed Δx_{tip} equal to 30 nm. For the sake of minimizing the beam divergence (u_t), the center of G_{col} was also shifted by Δx_{col} equal to 30 nm. We assumed that the incident optical field is polarized in the x -direction and illuminates the emitter vertically.

For the particle tracking simulation, we used a solver (CST Particle Studio³⁴⁾) that discretizes the emitter model by an adaptive hexahedral meshing with the number of mesh cells up to 8×10^7 . The distribution J_{ini} of the electron flux at the emitter apex generated by the laser illumination was calculated separately from the combination of the excitation light intensity obtained from the electromagnetic simulation described above and the electron flux density P_t obtained from the Fowler–Nordheim current density³⁵⁾ determined

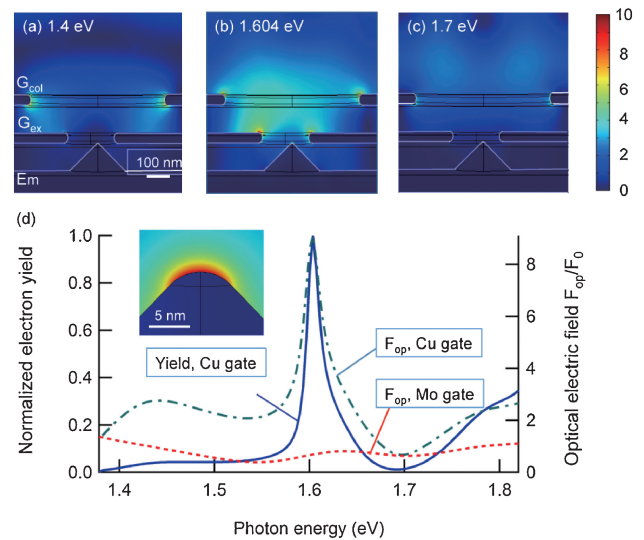


Fig. 2. Cross-sectional optical electric field distributions of a 750-nm-pitch molybdenum-tip array with the copper double-gate electrode under vertical incident laser irradiation on the $y = 0$ plane for the photon energies of (a) 1.4, (b) 1.6, and (c) 1.7 eV. Note the 30 nm shift of the emitter and the collimation gate in the x -direction. (d) Relation between yield of electrons generated by laser illumination and photon energy, normalized by the peak value at E_{ph} of 1.6 eV. The ratio of the optical electric field F_{op} at the tip apex center to the field F_0 of the incident light field is also shown for structures with copper gate (dash-dotted line) and molybdenum gate (dotted line). The color scale of F_{op} is indicated at the top right.

from the electrostatic field F_{dc} and barrier height Φ equal to $(W - E_{\text{ph}})$ (W of 4.5 eV is the work function of molybdenum and E_{ph} is the photon energy of the exciting laser) by assuming a uniform excited electron distribution.³⁶⁾ F_{dc} was calculated by using an adaptive tetragonal mesh three-dimensional finite element solver (COMSOL Multiphysics³¹⁾). Anticipating the maximum F_{dc} of 6 GV/m at the tip apex under the maximally collimated beam condition as in the previous laser-induced field emission experiment,¹⁹⁾ we set V_{ge} to 70 V and V_{col} to -76 V [see Fig. 1(b)]. We note that this simulation procedure was applied previously for a $2 \mu\text{m}$ base emitter double-gate structure³⁰⁾ that showed an excellent agreement with experiment.

Figures 2(a)–2(c) show the distribution of the optical electric field, when E_{ph} of the normal incident light field is equal to 1.4, 1.6, and 1.7 eV, respectively, along the $y = 0$ plane, which goes through the center of the shifted emitter. These show that the incident light field with E_{ph} of 1.6 eV resonantly propagated into the emitter cavity and enhanced F_{op} at the tip apex at the same time. This resonant behavior shows that EOT through the double-gate aperture holes is conserved in the presence of the molybdenum emitter. This directly extends the same effect proposed for single gold gate FEAs.²⁰⁾ Importantly, F_{op} at the tip apex should be larger than the incident field F_0 by a factor of ~ 9 to achieve the NIR laser-excited electron yield of $\sim 10^{-6}$ (see below). As shown in Fig. 2(d), right ordinate, this condition is achieved at the resonance. Further, as shown in the inset, the distribution of the enhanced F_{op} at the emitter tip is symmetric around the emitter tip axis despite the structural asymmetry caused by the finite Δx_{tip} . This is advantageous for minimizing u_t at the optimum collimation (see below).

In Fig. 2(d), we display the electron yield Y_{op} obtained by integrating J_{ini} over the apex surface at each E_{ph} . This shows that Y_{op} and F_{op} have nearly identical E_{ph} dependence. As a comparison, we also calculated the optical electric field distribution of the same double-gate emitter but when both gate electrodes consist of molybdenum (green dash-dotted line). The lack of the enhancement of the F_{op} -to- F_0 ratio in the Mo gate emitter clearly indicates the importance of the SPP resonance for the F_{op} increase of the copper gate emitter.

The maximum F_{op} -to- F_0 ratio of the copper double-gate emitter equal to 9 is approximately the same as the F_{op} -to- F_0 ratio equal to 9.5 for a 5- μ m-pitch single-Mo-gate emitter with R_{tip} of 5 nm (irradiated from 60°, not shown). This indicates that when F_{dc} and the intensity of the illuminating laser are the same, both emitters generate the same number of electrons per tip. Therefore, the electron yield of the 0.75- μ m-pitch double-Cu-gate array is expected to be higher than that of the 5- μ m-pitch array by a factor of 44 owing to the increased tip density. As a result, combining with the empirical electron yield (6×10^{-8}) of the 5- μ m-pitch array,¹⁹⁾ we estimate the electron yield of the 0.75- μ m-pitch Cu-double-gate emitter to be equal to 2×10^{-6} when it is excited at the resonance photon energy of 1.6 eV. This leads to the possibility of generating 200 pC electron pulses from a 10^6 -tip FEA with the array diameter of 1 mm by exciting the FEA with NIR laser pulses with the beam energy of ~ 0.1 mJ.

By using the J_{ini} calculated from F_{op} at the resonance (photon energy of 1.6 eV) and F_{dc} , we performed the particle tracking simulation with 10^4 particles. In Fig. 3(a), we show the relation between the velocity v_x in the x -direction and the position x of the particles (x -phase space) at the anode plane for V_{col} of 0, -76, -82, and -90 V. V_{ge} was fixed at 70 V. This shows that the v_x -spread was substantially reduced by decreasing V_{col} from 0 to -76 V, and then increased at -90 V due to the overfocusing. The closeness of the tip to G_{ext} in the positive x -direction deformed the x -phase space in the positive x side. However, the y -phase space stayed symmetric as shown in Fig. 3(b) ($V_{col} = -76$ V). Figure 3(c) depicts the electron orbits at V_{col} of -76 V observed along the $y = 0$ plane. For display purpose, a limited number of orbits are shown in the figure. This demonstrates that the diverging orbits near the emitter apex are collimated after the electrons pass through the G_{col} aperture. Figure 3(d) summarizes u_t calculated at various V_{col} values. The horizontal line indicates u_t equal to u_{th} of $4 \times 10^{-4} c$, which is the boundary; below this level, the estimated beam emittance for 1-mm-diameter FEA is less than 0.1 mm-mrad and more than a factor of 2 lower than that of the state-of-the-art photocathode.¹⁰⁾ Despite the asymmetry of the emitter structure, it predicts that u_t is below u_{th} for V_{col} between -72 and -82 V. The finite Δx_{tip} also introduced the finite mean v_x and the tilt of the beam in the x -direction at zero V_{col} . However, when the collimation condition is optimum, this is reduced to a value much less than u_{th} , and its effect becomes negligible.

The compatibility with the high acceleration field is an important issue for the use of FEAs in accelerators. Experimentally, stable operation of single-gate FEAs under acceleration up to 30 MV/m in 100-ns-pulse high-voltage diode gun was demonstrated.¹⁶⁾ Also, a recent publication by

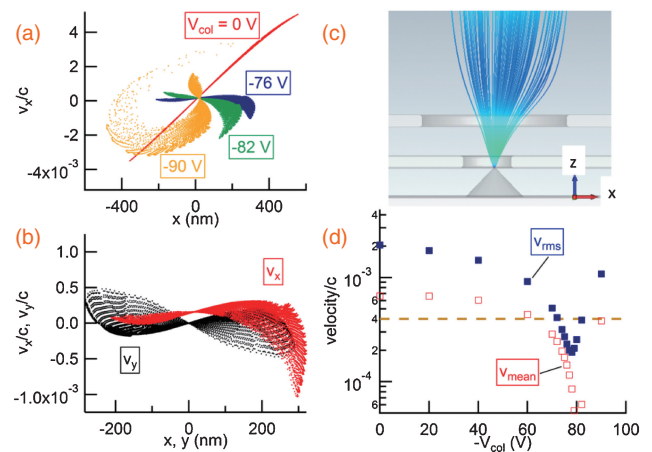


Fig. 3. (a) and (b) show the phase space of the laser-induced electron pulse from the Cu double-gate Mo-tip array in the x -direction on the plane at 1.5 μ m above G_{col} with the electron extraction potential of 70 V and acceleration field of 100 MV/m. (a) Phase space in x -direction at V_{col} of 0, -76, -82, and -90 V. (b) Phase space in x - and y -directions at V_{col} of -76 V. (c) Trajectories of small number of electrons at V_{col} of -76 V (the cross section is along $y = 0$ plane). (d) Variation of rms transverse velocity u_t (filled square) and mean velocity (open square) of the laser-induced field emission beam with the decrease of V_{col} from 0 to -80 V. The broken line indicates u_t equal to $4 \times 10^{-4} c$ with the corresponding intrinsic beam emittance of 0.1 mm-mrad for a 1 mm-diameter cathode.

Li et al.³⁷⁾ has reported a stable operation of nanostructured copper cathode in an RF cavity gun with the maximum acceleration field of 70 MV/m. These results indicate that stable operation of the nanofabricated FEAs in the actual gun environment is possible. Therefore, the test of FEAs in the actual RF gun environment is an interesting next step of research.

In the report of Li et al.,³⁷⁾ they utilized the SPP resonance of the nanostructure copper surface to enhance the multi-photon photoemission excited by femtosecond NIR laser pulses. The similar SPP effect is observed also in our simulation: F_{op} at the gate aperture edge was enhanced at the SPP resonance condition [Fig. 2(b)]. At the G_{ex} edges, the multi-photon photoemission is likely to be negligible under the operation condition of the double-gate FEAs since the DC fringe field from the gate potential increases the barrier height at the G_{ex} aperture edge and inhibits the electron emission.^{18,19)} The multiphoton photoemission from the G_{col} layer can also be substantially reduced by exciting the FEA with laser pulses with durations more than 10 times longer than 50 fs with the same pulse energy of ~ 0.1 mJ for 200 pC generation.

The impact of the space-charge effect on the electron propagation and the emittance is other important subject because of the plurality of the FEA beam.¹⁴⁾ We therefore repeated the particle track simulation assuming static tip current up to 200 μ A at V_{col} of -78 V with V_{ge} of 70 V and F_{acc} of 100 MV/m. We found that the increase of u_t is negligible up to the tip current of 20 μ A (corresponding to 10 ps pulse beam for 200 pC electron charge generation from a 10^6 -tip FEA). When the tip current is increased to 200 μ A (corresponding to the 1 ps FEA pulse case), u_t increases to $4 \times 10^{-4} c$. Further analysis in the case of transient and pulsed current propagation as well as the case with different device geometries may lead to more optimized performance

and operation condition. Therefore, it is also an important future research direction.

In summary, we studied the feasibility of stacked double-gate FEAs for advanced accelerator applications. Our simulation showed that, by engineering the device structure to effectively couple the NIR excitation of the SPP of the gate to the emitter tip, NIR laser pulses with pulse energies in the order of 0.1 mJ can generate 200 pC electron pulses with the intrinsic emittance below 0.1 mm-mrad from 10^6 -tip FEAs with the array diameter of 1 mm. We consider that actual fabrication of such shifted-tip double-gate emitter arrays is feasible; Recent report on the prototype submicron pitch single-gate FEAs³⁸⁾ showed that tip-gate alignment precision over 1 mm diameter by electron beam lithography is below a few nanometers. Hence these FEAs are highly promising for future accelerator applications and X-ray FELs that require ultra-high-brightness and high-current electron beams.

Acknowledgment The authors acknowledge Professor J. F. van der Veen for critical reading of the manuscript. This work was conducted within the SwissFEL project at the Paul Scherrer Institute and was partially supported by the Swiss National Science Foundation Nos. 200020_143428 and 2000021_147101.

- 1) A. V. Crewe, J. Wall, and J. Langmore: *Science* **168** (1970) 1338.
- 2) C. A. Brau: *Nucl. Instrum. Methods* **407** (1998) 1.
- 3) B. D. Patterson, R. Abela, H.-H. Braun, U. Flechsig, R. Ganter, Y. Kim, E. Kirk, A. Oppelt, M. Pedrozzi, S. Reiche, L. Rivkin, T. Schmidt, B. Schmitt, V. N. Strocov, S. Tsujino, and A. F. Wrulich: *New J. Phys.* **12** (2010) 035012.
- 4) W. S. Graves, F. X. Kärtner, D. E. Moncton, and P. Piot: *Phys. Rev. Lett.* **108** (2012) 263904.
- 5) H. Makishima, S. Miyano, H. Imura, J. Matsuoka, H. Takemura, and A. Okamoto: *Appl. Surf. Sci.* **146** (1999) 230.
- 6) K. B. K. Teo, E. Minoux, L. Hudanski, F. Peauger, J.-P. Schnell, L. Gangloff, P. Legagneux, D. Dieumegard, G. A. J. Amaratunga, and W. I. Milne: *Nature* **437** (2005) 968.
- 7) J. H. Booske: *Phys. Plasmas* **15** (2008) 055502.
- 8) D. R. Whaley, R. Duggal, C. M. Armstrong, C. L. Bellew, C. E. Holland, and C. A. Spindt: *IEEE Trans. Electron Devices* **56** (2009) 896.
- 9) SwissFEL Conceptual Design Report, PSI Bericht Nr. 10-04 April 2012 (<http://www.swissfel.ch>), p. 21.
- 10) Y. Ding, A. Brachmann, F.-J. Decker, D. Dowell, P. Emma, J. Frisch, S. Gilevich, G. Hays, Ph. Hering, Z. Huang, R. Iverson, H. Loos, A. Miahnahri, H.-D. Nuhn, D. Ratner, J. Turner, J. Welch, W. White, and J. Wu: *Phys. Rev. Lett.* **102** (2009) 254801.
- 11) P. R. Schwoebel, C. A. Spindt, and C. E. Holland: *J. Vac. Sci. Technol. B* **23** (2005) 691.
- 12) C. Li, Y. Zhang, M. T. Cole, S. G. Shivareddy, J. S. Barnard, W. Lei, B. Wang, D. Pribat, G. A. J. Amaratunga, and W. I. Milne: *ACS Nano* **6** (2012) 3236.
- 13) J. D. Jarvis, H. L. Andrews, C. A. Brau, J. Davidson, B. Ivanov, W.-P. Kang, C. L. Stewart, and Y.-M. Wong: Proc. FEL2009, 2009, WEOA04.
- 14) M. Dehler, A. Candel, and E. Gjonaj: *J. Vac. Sci. Technol. B* **24** (2006) 892.
- 15) K. L. Jensen, P. G. O'Shea, D. W. Feldman, and J. L. Shaw: *J. Appl. Phys.* **107** (2010) 014903.
- 16) S. Tsujino, M. Paraliiev, E. Kirk, T. Vogel, F. Le Pimpec, C. Gough, S. Ivkovic, and H.-H. Braun: *J. Vac. Sci. Technol. B* **29** (2011) 02B117.
- 17) J. D. Jarvis, B. K. Choi, A. B. Hmelo, B. Ivanov, and C. A. Brau: *J. Vac. Sci. Technol. B* **30** (2012) 042201.
- 18) S. Tsujino, P. Beaud, E. Kirk, T. Vogel, H. Sehr, J. Gobrecht, and A. Wrulich: *Appl. Phys. Lett.* **92** (2008) 193501.
- 19) A. Mustonen, P. Beaud, E. Kirk, T. Feurer, and S. Tsujino: *Appl. Phys. Lett.* **99** (2011) 103504.
- 20) A. Mustonen, P. Beaud, E. Kirk, T. Feurer, and S. Tsujino: *Sci. Rep.* **2** (2012) 915.
- 21) T. W. Ebbesen, H. J. Lezec, H. F. Ghaemi, T. Thio, and P. A. Wolff: *Nature* **391** (1998) 667.
- 22) M. Krüger, M. Schenk, and P. Hommelhoff: *Nature* **475** (2011) 78.
- 23) H. Yanagisawa, M. Hengsberger, D. Leuenberger, M. Klöckner, C. Hafner, T. Greber, and J. Osterwalder: *Phys. Rev. Lett.* **107** (2011) 087601.
- 24) G. Herink, D. R. Solli, M. Gulde, and C. Ropers: *Nature* **483** (2012) 190.
- 25) W. D. Kesling and C. E. Hunt: *IEEE Trans. Electron Devices* **42** (1995) 340.
- 26) J. Itoh, Y. Tohma, K. Morikawa, S. Kanemaru, and K. Shimizu: *J. Vac. Sci. Technol. B* **13** (1995) 1968.
- 27) C.-M. Tang, A. C. Ting, and T. Swyden: *Nucl. Instrum. Methods Phys. Res., Sect. A* **318** (1992) 353.
- 28) Y. Neo, M. Takeda, T. Soda, M. Nagao, T. Yoshida, S. Kanemaru, T. Sakai, K. Hagiwara, N. Saito, T. Aoki, and H. Mimura: *J. Vac. Sci. Technol. B* **27** (2009) 701.
- 29) P. Helfenstein, E. Kirk, K. Jefimovs, T. Vogel, C. Escher, H.-W. Fink, and S. Tsujino: *Appl. Phys. Lett.* **98** (2011) 061502.
- 30) P. Helfenstein, V. A. Guzenko, H.-W. Fink, and S. Tsujino: *J. Appl. Phys.* **113** (2013) 043306.
- 31) COMSOL Multiphysics [<http://www.comsol.com>].
- 32) *Handbook of Optical Constants of Solids*, ed. E. D. Palik (Academic Press, London, 1998).
- 33) L. Novotny, R. X. Bian, and X. S. Xie: *Phys. Rev. Lett.* **79** (1997) 645.
- 34) CST - Computer Simulation Technology [<http://www.cst.com>].
- 35) R. G. Forbes and J. H. B. Deane: *Proc. R. Soc. A* **463** (2007) 2907.
- 36) M. J. G. Lee: *Phys. Rev. Lett.* **30** (1973) 1193.
- 37) R. K. Li, H. To, G. Andonian, J. Feng, A. Polyakov, C. M. Soby, K. Thompson, W. Wan, H. A. Padmore, and P. Musumeci: *Phys. Rev. Lett.* **110** (2013) 074801.
- 38) V. A. Guzenko, A. Mustonen, P. Helfenstein, E. Kirk, and S. Tsujino: *Microelectron. Eng.* **111** (2013) 114.